DOI: 10.1002/cmdc.200600015

A Fluorine Scan at the Catalytic Center of Thrombin: C–F, C–OH, and C–OMe Bioisosterism and Fluorine Effects on pK_a and log *D* Values

Eliane Schweizer,[a] Anja Hoffmann-Röder,[b] Kaspar Schärer,[a] Jacob A. Olsen,[a] Christoph Fäh,[a] Paul Seiler,[a] Ulrike Obst-Sander,[c] Björn Wagner,[c] Manfred Kansy,[c] and François Diederich*[a]

A series of 16 tricyclic thrombin inhibitors was prepared by using the 1,3-dipolar cycloaddition of azomethine ylides derived from 3- or 4-hydroxyproline and 4-bromobenzaldehyde, with N-*(4-fluorobenzyl)maleimide as the key step. The terminal pyrrolidine ring of the inhibitors was systematically substituted to explore the potential bioisosteric behavior of C–F, C–OH, and C–OMe residues pointing into the environment of the catalytic center of a serine protease. X-ray crystal structure analyses revealed a distinct puckering preference of this ring. Substitution by F, HO, and MeO has a strong effect on the basicity of the adjacent pyrrolidine nitrogen center which originates from two* σ*-inductive pathways between this center and the electronegative O and F atoms.* gem*-Difluorination decreases the* pK_a *value of this tertiary amine center to* <2*, making the conjugated ammonium ion a moderately strong acid. Unexpectedly, F substitution next to the nitrogen center reduced the lipophilicity of the ligands, as revealed by measurements of the logarithmic partition coefficient log* D*. The biological assays showed that all compounds are thrombin inhibitors with activities between* $K_i = 0.08$ *and 2.17* μM*. Bioisosteric behavior of F, HO, and MeO substituents was observed. Their electronegative F and O atoms undergo energetically similar polar interactions with positively polarized centers, such as the N atom of His 57 which is hydrogen bonded to the catalytic Ser 195. However, for energetically similar polar interactions of C–F, C–OH, and C–OMe to occur, sufficient space is necessary for the accommodation of the Me group of the C–OMe residue, and a H-bond acceptor must be present to prevent unfavorable desolvation of the C–OH residue.*

Introduction

In view of the eminent role of organofluorine in medicinal chemistry[1] and crop protection,[2,3] we started a fluorine scan on tricyclic thrombin inhibitors a few years ago,[4] systematically exchanging H for F substituents to map the fluorophilicity/fluorophobicity of an entire enzyme active site.[5,6] Thrombin was chosen for this investigation because its active site has limited conformational flexibility, and several X-ray crystal structures have shown nearly identical binding geometries for different inhibitors with the tricyclic core, which is important for meaningful structure–activity relationships. Systematic fluorination of the benzyl ring reaching into the distal (D) pocket (Figure 1) led to the discovery of orthogonal multipolar C–F···C=O interactions,[5a,b,7a] which were later shown by model studies to be attractive.[7b] Introduction of fluorine into the phenylamidinium residue that occupies the selectivity (S1) pocket reduced its pK_a value, and also affected inhibitory potency.[5c] Moreover, linear free-energy relationships revealed that the binding to thrombin became much weaker with decreasing pK_a values than the binding to the related serine protease trypsin, leading to an undesirable and unexpected loss in selectivity.[8]

Herein, we report the systematic substitution of the proline-derived ring of the tricyclic inhibitor core by F, HO, and MeO at position 7 directed towards His 57 and Ser 195 of the catalytic triad, and at position 8 situated above the oxyanion hole (Figure 1). The impact of these substitutions on biological activity and physicochemical properties (pK_a and log *D*) was also investigated. A survey of structural chemistry and biology databases[7a] (Cambridge Structural Database (CSD) and Protein Da-

[a] *E. Schweizer, Dr. K. Schärer, Dr. J. A. Olsen, C. Fäh, P. Seiler, Prof. Dr. F. Diederich*
Laboratorium für Organische Chemie, ETH Zürich, Hönggerberg, HCI
8093 Zürich (Switzerland)
Fax: (+41) 1-632-1109
E-mail: diederich@org.chem.ethz.ch

[b] *Dr. A. Hoffmann-Röder*
Institut für Organische Chemie, Johannes Gutenberg-Universität
Duesbergweg 10-14, 55128 Mainz (Germany)

[c] *Dr. U. Obst-Sander, Dr. B. Wagner, Dr. M. Kansy*
Pharma Research Basel, Discovery Chemistry
F. Hoffmann-La Roche Ltd, 4070 Basel (Switzerland)

Supporting information for this article is available on the WWW under http://www.chemmedchem.org or from the author.

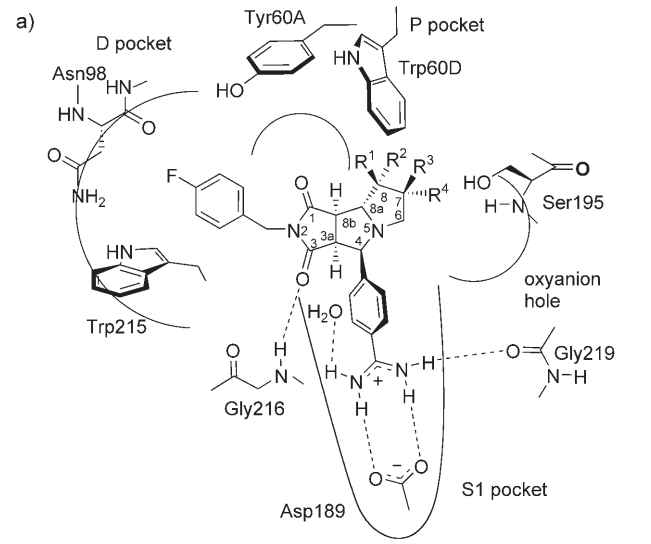

b)

	R^1	R^2	R^3	R^4
(±)-**1**	H	H	H	H
(+)-**2**	OH	H	H	H
(+)-**3**	OMe	H	H	H
(+)-**4**	F	H	H	H
(+)-**5**	H	OH	H	H
(+)-**6**	H	OMe	H	H
(+)-**7**	H	F	H	H
(+)-**8**	F	F	H	H
(+)-**9**	OMe	OMe	H	H
(+)-**10**	H	H	OH	H
(+)-**11**	H	H	OMe	H
(+)-**12**	H	H	F	H
(+)-**13**	H	H	H	OH
(+)-**14**	H	H	H	OMe
(+)-**15**	H	H	H	F
(±)-**16**	H	H	F	F
(±)-**17**	H	H	OMe	OMe

Figure 1. a) Representation of the binding mode of the tricyclic inhibitors in the active site of thrombin. The active site is defined by the catalytic center with the nucleophilic Ser195 and the oxyanion hole, the selectivity (S1) pocket, the large hydrophobic distal (D) pocket, and a small proximal (P) pocket. b) Inhibitors **1**–**17** prepared to explore C–F, C–OH, and C–OMe bioisosterism in the environment of the catalytic center of thrombin. In the case of racemates, only the (3a*S*,4*R*,8a*S*,8b*R*)-configured enantiomer is bound.[4,5]

tabank (PDB)) revealed that C–F, C–OH, and C–OMe groups undergo similar orthogonal multipolar interactions with C=O residues, suggesting possible bioisosteric behavior of the three residues.[9]

Bioisosteric substitution of functional groups is a well-established strategy in medicinal chemistry to optimize potency, selectivity, and the ADME (absorption, distribution, metabolism, and excretion) profile of a given lead compound during the quest for potential drug candidates. In general, the concept of bioisosterism refers to a set of atoms or groups that share similar shapes, volumes, electronic distributions, and physicochemical properties, which together lead to similar biological activities.[10] Numerous bioisosteric relationships have been identified but chemists often use such transformations intuitively, and no definite classification of the biological effects of each structural change can be made. Two specific residues show bioisosteric character within one receptor site, but may behave differently within another receptor site.[10a] Nevertheless, the basis for quantitative structure–activity relationships (QSAR) in drug development has been set by bioisosteric substitutions which frequently provide a specific insight into pharmacophoric sites for rational drug design.[11]

Results and Discussion

Synthesis of the inhibitors

The synthesis of the racemic ligands (±)-**1**, (±)-**16**, and (±)-**17**, and the optically pure derivatives (+)-**2**–(+)-**15** (Figure 1) was carried out according to a previously published protocol developed in our research group.[4] Characteristic examples are shown in Schemes 1–3 (see also the Supporting Information). Starting from readily available *N*-(4-fluorobenzyl)maleimide (**18**),[5b] commercial 4-bromobenzaldehyde (**19**), and *trans*-3-hydroxy-L-proline (**20**) or *trans*-4-hydroxy-L-proline (**21**), the tricyclic inhibitor scaffold was assembled by azomethine ylide 1,3-dipolar cycloaddition. Whereas both cycloadducts (+)-**22** and (−)-**23** from the reaction of 3-hydroxyproline **20** were easily separated by column chromatography (CC) from their diastereomeric congeners, two pairs of inseparable *pseudoenantiomers*[4c] (+)-**24**/(−)-**25** and (+)-**26**/(−)-**27** were obtained from the corresponding transformation with 4-hydroxyproline **21**. However, the desired cycloadduct (+)-**24** was isolated in enantiomerically pure form after protection of alcohols (+)-**24**/(−)-**25** as TBDMS ethers, and chromatographic separation of the two diastereoisomers (+)-**28** and (−)-**29**, followed by desilylation of (+)-**28** (Scheme 1).

The exchange of the HO group for F and MeO, as shown for adduct (+)-**22** (Scheme 2), was accomplished after conversion of the aromatic bromide into the corresponding nitrile (+)-**30**. Subsequent deoxyfluorination and inversion of configuration with DAST[12] yielded the desired monofluoride (+)-**31**. Treatment of (+)-**30** with NaH/MeI furnished the methylated precursor (+)-**32**. Nitriles (+)-**30**, (+)-**31**, and (+)-**32** were subsequently transformed in a Pinner reaction[13] into the desired amidinium salts (+)-**2**, (+)-**7**, and (+)-**3**, respectively. For the preparation of the corresponding inhibitors with inverted configurations at C8 and for the target molecules substituted at C7, a similar route, preceded by a Mitsunobu reaction[14] with (+)-**30** was followed (Supporting Information).

The synthesis of the difluoro- and dimethoxy-substituted inhibitors (+)-**8** and (+)-**9**, starting from nitrile (+)-**30**, required an oxidation step to the corresponding ketone (+)-**33** (Scheme 3). Double deoxyfluorination to nitrile (+)-**34** with DAST (Scheme 3), followed by the Pinner reaction, furnished inhibitor (+)-**8**, while acetal (+)-**9** was directly obtained from ketone (+)-**33** during the formation of the amidinium salt. Acetals (+)-**9** and (±)-**17** were found to be remarkably stable even under the conditions of the biological assay (see below).

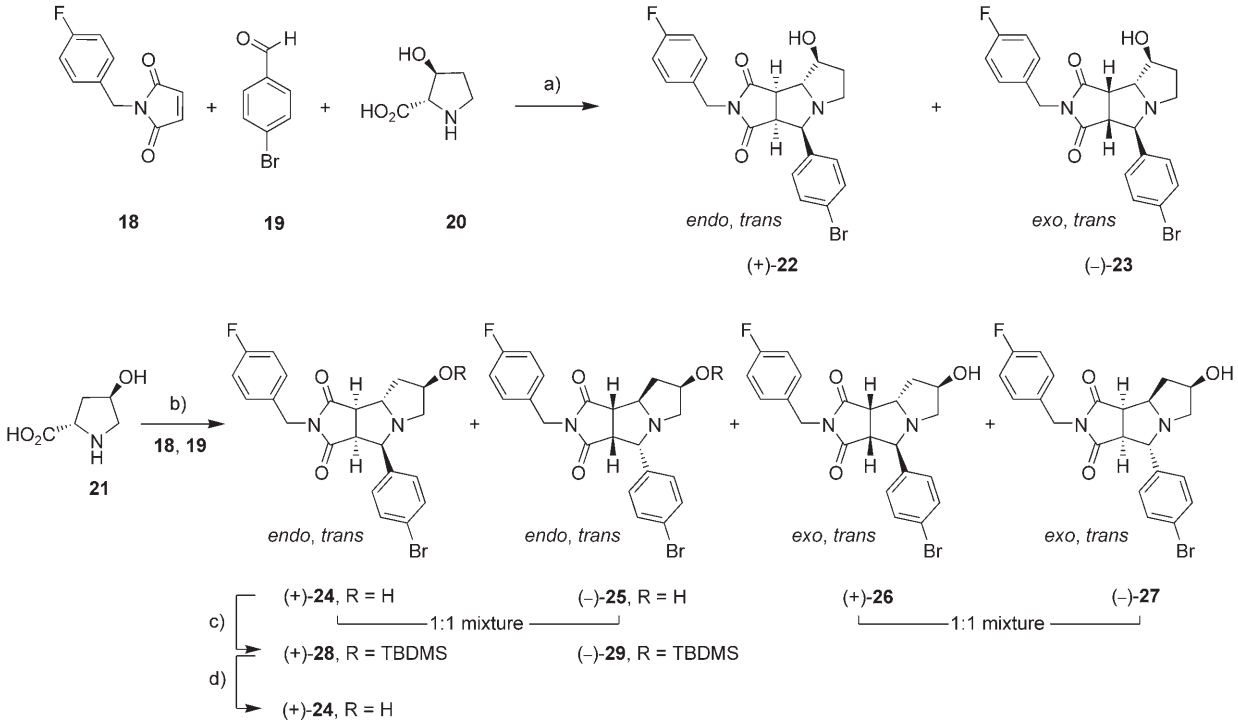

Scheme 1. Synthesis of the intermediates (+)-**22** and (+)-**24**: a) MeCN, 80 °C, 18 h, (+)-**22** (24%), (−)-**23** (30%); b) DMF, 80 °C, 48 h, (+)-**24**/(−)-**25** (47%), (+)-**26**/(−)-**27** (35%); c) TBDMS Cl, DMAP, NEt_3, CH_2Cl_2, 25 °C, 35 h, (+)-**28** (31%), (−)-**29** (42%); d) nBu$_4$NF, THF, 0 °C→25 °C, 90 min, 82%. TBDMS = *tert*-butyldimethylsilyl; DMAP = 4-(dimethylamino)pyridine. Only *endo*, *trans* adducts lead to active inhibitors.[4] *Exo* and *endo* refer to the orientation of the 4-bromophenyl substituent at C4 with respect to the bicyclic perhydropyrrolo[3,4-c]pyrrole scaffold, and *cis* and *trans*, to the position of this 4-bromophenyl ring with respect to the configuration of C8a at the fusion of the two 5-membered rings in the perhydropyrrolizidine bicycle (for atom numbering, see Figure 1).

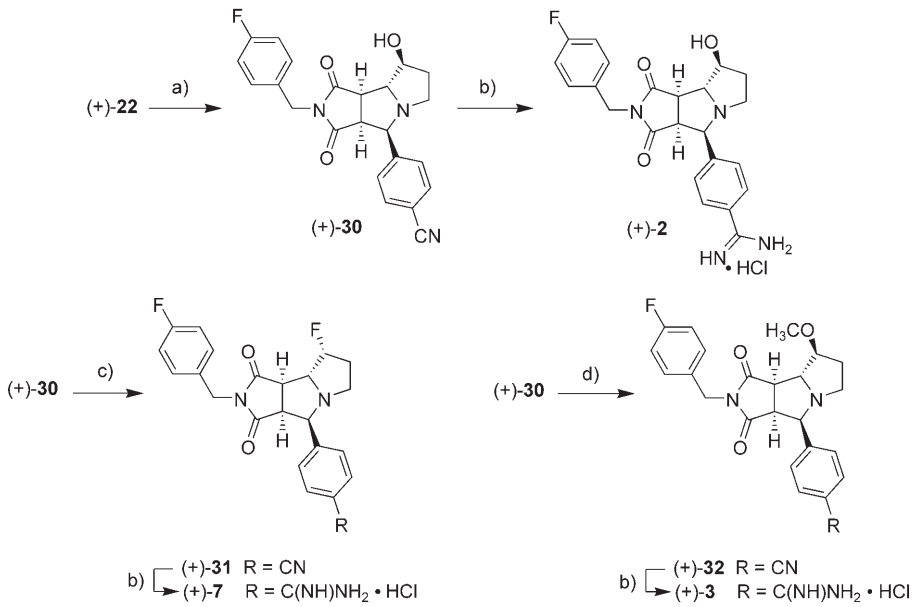

Scheme 2. Synthesis of the inhibitors (+)-**2**, (+)-**3**, and (+)-**7**: a) [Pd_2(dba)$_3$], dppf, $Zn(CN)_2$, DMF, 120 °C, 16 h, 91%; b) 1) MeOH, HCl (g), CH_2Cl_2, 4 °C, 28–35 h; 2) NH_3, MeOH, 65 °C, 3 h, (+)-**2** (66%), (+)-**7** (58%), (+)-**3** (56%); c) DAST, CH_2Cl_2, −78 °C→25 °C, 2 h, 79%; d) NaH, MeI, THF, 25 °C, 2 h, 27%. Dppf = diphenylphosphinoferrocene, DMF = *N*,*N*-dimethylformamide, DAST = diethylaminosulfur trifluoride.

X-ray crystallography

X-ray crystal structure analyses were obtained for intermediates (+)-**22**, (+)-**34**, (+)-**36**, and (+)-**39,** ORTEP plots and visualizations of close next-neighbor interactions in the crystal packing are shown in the Supporting Information. Figure 2a shows the four structures superimposed around the central 5-membered ring of the tricyclic skeleton. Interestingly, the same pucker in the terminal pyrrolidine ring is maintained, independent of the nature and pattern of substitution. This pucker differs from the one seen in the crystal structures of tricyclic inhibitors bound to thrombin.[4,5] In four of these co-crystal structures (Supporting Information), the nearly planar torsional angle shifts from τ_4 (Figure 2) to τ_2 (−9°–3°) and in the fifth to τ_1 (−1°). These puckers, determined from the observed electron density, allow a better fit of the inhibitors in the thrombin active site, as suggested by molecular modeling. Accordingly, all modeling simulations of the binding modes of the new inhibitors (see below) start from the known co-crystal structures.

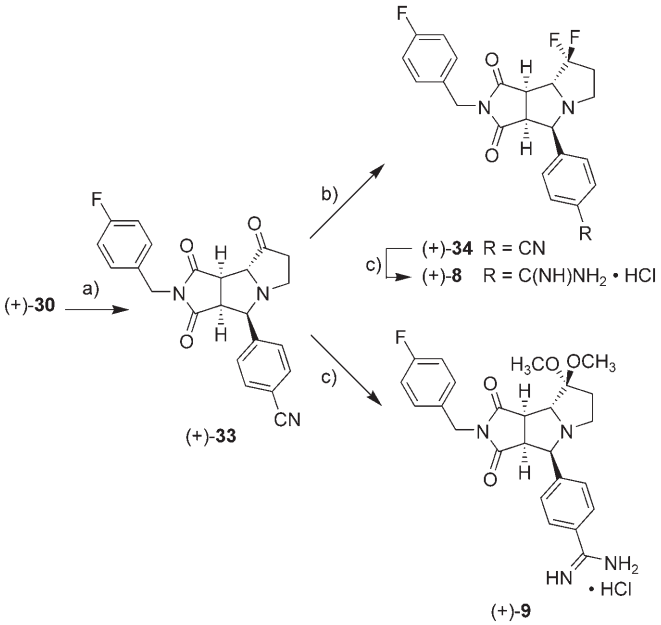

Scheme 3. Synthesis of the target compounds (+)-**8** and (+)-**9**: a) Dess–Martin periodinane, CH_2Cl_2, 25 °C, 3 h, 63%; b) DAST, CH_2Cl_2, −78 °C→25 °C, 2 h, 48%; c) 1) MeOH, HCl (g), CH_2Cl_2, 4 °C, 28–35 h; 2) NH_3, MeOH, 65 °C, 3 h, (+)-**8** (54%), (+)-**9** (31%).

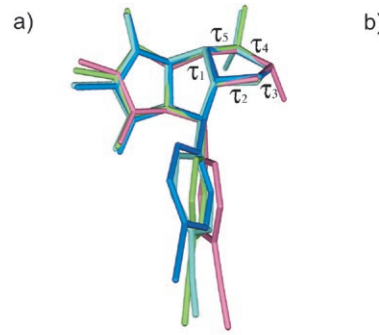

	τ_1	τ_2	τ_3	τ_4	τ_5	R^1	R^2	R^3	R^4
(+)-**22**	36°	-37°	23°	-1°	-22°	OH	H	H	Br
(+)-**34**	35°	-33°	18°	4°	-24°	F	F	H	CN
(+)-**36**	32°	-36°	26°	-5°	-16°	F	H	H	CN
(+)-**39**	35°	-35°	21°	1°	-22°	H	H	F	CN

Figure 2. a) Torsional angles (τ) of the terminal pyrrolidine ring of tricyclic inhibitors as determined by X-ray crystallographic analysis. The imide N substituents are omitted for clarity. Color code: (+)-**22**: blue, (+)-**34**: cyan, (+)-**36**: green, (+)-**39**: pink. b) Diagram of the same compounds (+)-**22**, (+)-**34**, (+)-**36**, and (+)-**39**, showing the R-group locations.

It is noticeable that a pucker similar to the one shown in Figure 2a is also seen in 10 (out of 16) crystal structures of related compounds, including a phenylamidinium inhibitor.[4,5] In all 16 cases, the nearly planar torsional angle differs from the one observed for the bound ligands.

Fluorine effects on pK_a values

The pK_a values of the inhibitors were determined by potentiometric titration as previously described (Table 1).[5c] Whereas

Table 1. Biological activities and physicochemical properties of thrombin inhibitors.

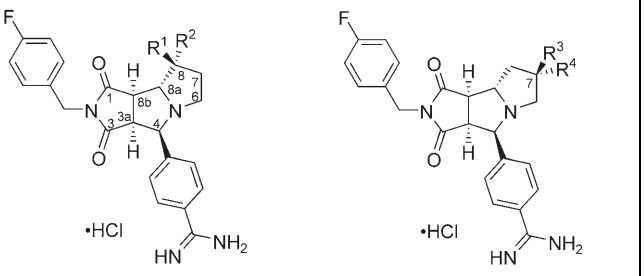

	R^1	R^2	K_i [μM][a]	Sel.[b]	pK_{a1}[c]	pK_{a2}[c]	log D[d]	C log P
(±)-**1**[e,f]	H	H	0.06	67	4.47	11.14	−1.16	1.99
(+)-**2**	OH	H	0.32	17	4.14	n.d.[g]	−0.91	1.36
(+)-**3**	OMe	H	0.28	16	3.68	11.20	−1.08	1.36
(+)-**4**	F	H	0.30	32	3.36	11.41[h]	−1.32	2.14
(+)-**5**	H	OH	2.17	19	4.19	11.28	−1.35	1.36
(+)-**6**	H	OMe	0.33	60	4.15	11.07	−1.07	1.36
(+)-**7**	H	F	0.45	22	3.34	11.22	−1.17	2.14
(+)-**8**	F	F	0.71	29	<2	10.97	−1.31	2.28
(+)-**9**	OMe	OMe	0.59	25	3.25	10.95	−1.08	1.01
	R^3	R^4	K_i [μM][a]	Sel.[b]	pK_{a1}[c]	pK_{a2}[c]	log D[d]	C log P
(+)-**10**	OH	H	0.12	28	3.85	11.09	<−1	0.74
(+)-**11**	OMe	H	0.13	22	3.64	10.90	−1.36	1.36
(+)-**12**	F	H	0.08	37	3.25	11.25	−1.55	1.99
(+)-**13**	H	OH	0.26	31	3.85	11.01	<−1	0.74
(+)-**14**	H	OMe	1.16	34	3.68	10.90	−1.04	1.36
(+)-**15**	H	F	0.63	19	3.27	11.19	−1.41	2.28
(±)-**16**[e]	F	F	0.59	48	<2	11.12	−1.01	2.28
(±)-**17**[e]	OMe	OMe	2.14	14	3.16	11.16	−1.03	1.01

[a] The uncertainty of the measured K_i values is ±20%. [b] Selectivity (Sel.) = K_i(trypsin)/K_i(thrombin). [c] pK_{a1}: Tertiary amine in the tricyclic core; pK_{a2}: phenylamidinium. Accuracy of the pK_a measurements: ±0.1 pK_a units. [d] Accuracy of the log D measurements: <±0.1 log D units. [e] Only the (3a*S*,4*R*,8a*S*,8b*R*)-configured enantiomer is bound, as determined from crystal structure analyses.[4a,b] [f] From Ref. [5c] [g] n.d. = not detectable due to poor UV absorption. [h] This comparatively high value is probably related to the instability of the compound.[5c]

the pK_a value of the phenylamidinium residue lies in the expected range (pK_{a2}, approximately 11), the value (pK_{a1}) for the tertiary amine center in the tricyclic scaffold is remarkably low,[5c] varying between <2 and 4.47, and is strongly affected by substitution of the terminal 5-membered ring. We attributed the low pK_{a1} value of (±)-**1** (4.47) to the σ-inductive effect of the phenylamidinium ring in the α-position with respect to the N atom, and to the poorly appreciated, large σ-inductive effects of the two imide C=O moieties in the β-position.[5c] Such σ-inductive effects are particularly effective in rigid systems such as the tricyclic core of our inhibitors.

Incorporation of the F, HO, and MeO substituents into the terminal pyrrolidine ring reduces the pK_{a1} value further, as the inductive effect is transmitted by two σ-paths. Each substituent X is in both a β- (N-C-CX) and a γ-position (N-C-C-CX) to the N atom. Several trends are noticeable: 1) the σ-inductive effect of fluorine is much stronger than that of the HO and MeO substituents (for example (+)-**10**: 3.9 (HO); (+)-**11**: 3.6 (MeO); (+)-**12**: 3.3 (F)); 2) the effects of HO and MeO can differ by ΔpK_{a1} =

0.5 ((+)-**2** versus (+)-**3**), but can also be quite similar ($\Delta pK_{a1} = 0.04$; (+)-**5** versus (+)-**6**); 3) the effects of the two *gem* substituents (F or MeO) are additive in our ligand system: thus the pK_{a1} value changes from <2 for (+)-**8** (2 F) and 3.3–3.4 for (+)-**4** and (+)-**7** (1 F), to 4.5 for (±)-**1** (0 F), or from 3.2 for (±)-**17** (2 MeO) and 3.6–3.7 for (+)-**11** and (+)-**14** (1 MeO), to 4.5 for (±)-**1** (0 MeO); and 4) whereas, the epimers with different configuration at C7 show nearly identical pK_{a1} values, those with different configuration at C8 can change substantially (for example (+)-**3**: 3.7 and (+)-**6**: 4.2). Substituents at C8 are more strongly influenced by the steric bulk of the tricyclic core, which could induce differential solvation, thus affecting the pK_{a1} value. σ-Conjugation will also be affected by the ring pucker. The pK_a-lowering effect of fluorine substituents on the amine centers is well known, and is used to modulate pharmacokinetic properties[1,15] such as metabolic stability and membrane permeability. The strong inductive effects of alkoxy substituents (such as MeO) is less appreciated, but holds promise for similar use in physical property modulation.

Inverse fluorine effects on log *D*

It is well established that H/F exchange increases the lipophilicity of a molecule.[1] The measurement of log *D* values (log *D* is the logarithmic coefficient of the distribution of a compound between octanol and water at pH 7.4) of nearly 300 compounds showed that substitution of an H atom by an F atom increases log *D* values, on average, by approximately 0.25.[1a] However, the authors observed some exceptions to this general trend. Fluorine in the vicinity of HO, RO, and C=O groups was found to lower the log *D* value. This was explained by an enhanced polarization of the neighboring oxygen atom, resulting in greater solvation in water. In contrast, fluorine in the vicinity of amine centers was found, in most cases, to increase log *D* values because of a lowering of the basicity of the nitrogen functionality.

We also expected that the σ-accepting HO, MeO, and F substituents introduced near the tertiary amine center would further decrease its basicity and therefore increase the molecular log *D* value. Indeed, calculated C log *P* values (log *P* is the octanol/water partition coefficient for the *neutral* molecule) were in agreement with earlier work,[1] and the C log *P* values increase with F-substitution (Table 1); for example, (+)-**2** (OH) and (+)-**3** (OMe) have a C log *P* values of 1.4, whereas (+)-**4** (F) has a C log *P* value of 2.1. In contrast, the log *D* values measured for most of the monofluorinated inhibitors are substantially lower than that for the unsubstituted inhibitor ((±)-**1**: $\log D = -1.2$). Thus, the values for the three monofluorinated inhibitors (+)-**4**, (+)-**12**, and (+)-**15** vary between −1.3 and −1.6, whereas the F atom in (+)-**7** has no effect. At present, we do not have a good explanation for this finding. However, it needs to be taken into consideration that the uncertainties of log *D* values below −1 are large due to experimental difficulties with their measurements. It is noticeable that the trend is not as homogeneous for the HO- or MeO-substituted ligands or for the difluoro derivatives. Difluoro compound (+)-**8** gives a more negative log *D* value (−1.3), whereas compound (±)-**16** (−1.0) gives a greater positive log *D* value. In agreement with the earlier study,[1] we suggest that caution needs to be applied in the use of F-atom substitution to increase lipophilicity. In particular, the effect of H/F-substitution in the vicinity of N,O heteroatoms on log *D* values seems to be unpredictable, which could result from molecule-specific solvent effects, conformational effects, or both.

Biological results

The inhibition constants K_i for the complexes of the new inhibitors with thrombin and trypsin were determined using a chromogenic substrate, as previously described (Table 1).[16] Most of the compounds are potent inhibitors of thrombin, with K_i values between 0.08 and 2.17 μM (Table 1). Whereas ligands (+)-**10**, (+)-**11**, and (+)-**12** are nearly as active as the control compound (±)-**1** containing the unsubstituted terminal pyrrolidine ring, most other derivatives are less potent. Their selectivity for thrombin over trypsin is moderate (factors of 14 to 67). We have shown[4,5] that tricyclic imide inhibitors with similar activities are readily transformed (by exchanging the "upper" imide C=O group with a suitably sized *exo*-oriented alkyl substituent (*i*Pr, Et) to fill the P pocket that is absent in trypsin) into much more potent tricyclic lactam inhibitors, with K_i values in the lower nanomolar range and selectivities up to 760.

The main purpose of this investigation, however, was not an optimization of binding potency but the exploration of similarities in the molecular recognition properties of F, HO, and MeO substituents in biological environments. In this respect, a series of remarkable results were obtained. In three of the four series of inhibitors ((+)-**2**–(+)-**4**, (+)-**5**–(+)-**7**, (+)-**10**–(+)-**12**, and (+)-**13**–(+)-**15**), differing only in the nature of one substituent on the terminal pyrrolidine ring, the binding potencies of the F, HO, and MeO derivatives are basically identical. A correlation of binding potency with log *D* is not observed; ligand (+)-**12** which has the lowest log *D* value, forms the most stable complex. Despite some distinct exceptions discussed below in more detail, HO, F and MeO substituents on the terminal ring of our tricyclic inhibitors feature bioisosteric behavior. Based on available X-ray crystallographic information for the conserved binding mode of these ligands,[4,5] we performed molecular modeling analyses using MOLOC[17] to interpret these findings.

Importantly, the modeling shows that in each of the four inhibitor series, all three substituents (F, HO, and MeO) can be docked into the thrombin active site without steric hindrance. Subsequent energy minimizations, keeping the crystal-structure-based protein conformation fixed (with one exception, discussed directly below), led to a similar positioning of the O and F atoms of the substituents in each series (Supporting Information), which is essential for a meaningful discussion of isosteric behavior. The substituents at C8 *trans* to the C8a-C8b bond in the equally potent ligands (+)-**2**–(+)-**4** point toward the Lys60 E side chain near the surface of the enzyme. To accommodate the bulkier MeO group, this side chain was relaxed and allowed to undergo a minor conformational change (the

flexibility of thrombin Lys60 E is well established).[16b,18] In the series of equally potent inhibitors (+)-**10**–(+)-**12**, the *trans* substituents (*trans* as defined above) point to the surface of the protein; nevertheless, these compounds are the best binders. In the *cis* series (+)-**13**–(+)-**15**, the substituents are located on top of the oxyanion hole. This polar region of the enzyme prefers occupation by the polar HO residue ((+)-**13**: 0.26 μM) rather than by F ((+)-**15**: 0.63 μM) or MeO ((+)-**14**: 1.16 μM) residues. This result confirms our previous findings that the polar oxyanion hole environment does not accommodate lipophilic residues well.[4c]

The most interesting case is provided by the *cis*-substituted inhibitors (+)-**5**–(+)-**7** (Figure 3). In complexes with thrombin, the F and O atoms of the substituents point toward the imidazole ring of His 57 in the catalytic triad. More specifically, these atoms approach the N atom of His 57 that accepts the proton from Ser 195 in an orthogonal fashion, and consequencely is strongly positively polarized. We propose that the O and F atoms of the substituents engage in an attractive polar interaction with this positively polarized N center. However, the biological assay shows that F-substituted (+)-**7** (0.45 μM) and MeO-substituted (+)-**6** (0.33 μM) are much better binders than HO-substituted (+)-**5** (2.17 μM). According to the modeling, the bulkier MeO substituent is well accommodated without any steric repulsions. In contrast, the HO group does not seem to find a H-bonding acceptor, as the neighboring catalytic Ser 195 forms the H-bond to His 57. Based on these results, which require further confirmation in other systems, we tentatively propose the following requirements for bioisosterism of C–F, C–OH, and C–OMe residues engaging with their electronegative atoms in multipolar interactions: similar interaction strength will only be gained if the bulky Me group of the MeO substituent can be accommodated without steric repulsions with the protein environment and if the H atom of the HO-group finds a H-bond acceptor. If the latter is not the case, unfavorable desolvation costs predominate, which presumably explains the weaker association of (+)-**5**. Finally, we note a similar binding strength of the *gem*-disubstituted pair (+)-**8** (2 F, 0.71 μM) and (+)-**9** (2 MeO, 0.59 μM), whereas the dimethoxy compound (±)-**17** (2.14 μM) is less potent than the difluoro derivative (±)-**16** (0.59 μM), because of the unfavorable location of the Me group in the polar oxyanion hole environment.

Conclusions

We have conducted a systematic exploration of the molecular recognition requirements for bioisosterism of C–F, C–OMe, and C–OH groups attached to the terminal pyrrolidine ring of tricyclic thrombin inhibitors and directed into the environment of the catalytic center of the serine protease. X-ray crystal structures of four compounds revealed a distinct puckering preference of this five-membered ring, different from the one observed in the enzyme co-crystals. Through two σ-inductive pathways, the substituents strongly decrease the basicity of the tertiary pyrrolidine nitrogen center, with fluorine effects expectedly being the strongest. In fact, upon *gem* difluorination, basicity is completely lost, and the conjugated ammonium ion becomes a moderately strong acid ($pK_{a1} < 2$). Unexpected results were obtained from measurements of log *D* as a parameter for the lipophilicity of the ligands at pH 7.4. F substitution in the neighborhood of the tertiary amine center does not increase, but instead decreases the log *D* value. The biological data clearly support the notion of bioisosteric behavior of C–F, C–OH, and C–OMe, particularly when their electronegative F and O atoms undergo polar interactions with a strongly positively polarized center such as the N atom of His 57, which accepts the H bond from the nucleophilic Ser 195 in the catalytic triad. However, for energetically similar interactions, the C–OMe residue requires more space for the bulky Me group and the C–OH residue needs to find a H-bond acceptor to prevent unfavorable desolvation. This investigation, similar to previous reports,[5] demonstrates the value of a systematic fluorine scan at an enzyme active site, which in turn leads to a greater understanding of molecular recognition and physical properties that will be useful far beyond the specific example of thrombin inhibition.

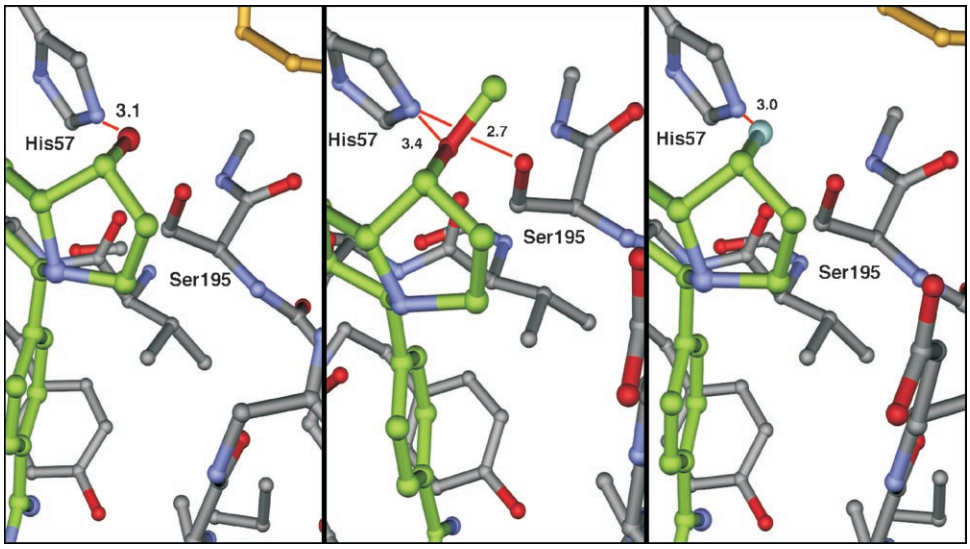

Figure 3. Polar interactions between the electronegative F and O atoms of the substituents of inhibitors (+)-**5** (left), (+)-**6** (middle), and (+)-**7** (right), and the positively polarized N atom of His 57 in the catalytic triad, as suggested by molecular modeling. Distances shown are in Å. Color code: C skeleton of the inhibitors: green, C skeleton of the protein: grey, O atoms: red, N atoms: blue, F atoms: light green, S atoms: yellow.

Experimental Section

General: Solvents and reagents were reagent grade, purchased from commercial suppliers, and used without further purification unless otherwise stated. THF was

freshly distilled from sodium benzophenone ketyl, CH_2Cl_2 from CaH_2. HCl gas was dried with concentrated H_2SO_4. If not mentioned otherwise, all products were dried under high vacuum (10^{-2} Torr) before analytical characterization. Column chromatography (CC): SiO_2-60 (230–400 mesh, 0.040–0.063 mm) from Fluka. TLC: SiO_2-60 F_{245} (on glass) Merck, visualization by UV light at 245 nm and staining with a solution of $KMnO_4$ (1.5 g), K_2CO_3 (10 g), 5% NaOH (2.5 mL) in H_2O (150 mL); a solution of anisaldehyde (6.8 mL), concentrated H_2SO_4 (9.2 mL), and acetic acid (2.8 mL) in EtOH (250 mL); or a solution of ninhydrin (0.3 g) in butanol (100 mL) and glacial acetic acid (3 mL). Melting points: Büchi-510 apparatus; uncorrected. IR spectra: Perkin–Elmer Spectrum BX FTIR System spectrometer (ATR-unit, Golden Gate). NMR spectra (^1H, ^{13}C, ^{19}F): Varian Gemini-300, Varian Gemini-400, Bruker ARX-300, and Bruker AMX-500; spectra were recorded at 25 °C with solvent peak or $CFCl_3$ as reference. In the ^{13}C NMR spectrum of compounds (+)-**3** and (+)-**9**, three and two resonances, respectively, overlap or are buried under the solvent peak. The exchangeable amidinium protons were not observed in ^1H NMR spectra recorded in CD_3OD. High-resolution MALDI mass spectra (HRMS): IonSpec Ultima, 2,5-dihydroxybenzoic acid (DHB) as matrix; molecular ions (M^+) reported for phenylamidinium salts refer to the corresponding phenylamidine derivatives. Elemental analyses were performed by the Mikrolabor at the Laboratorium für Organische Chemie, ETH Zürich. The nomenclature was generated with the computer programs AUTONOM (Beilstein) and ACD-Name (ACD/Labs).

Determination of inhibition constants: The affinity of thrombin inhibitors was determined according to previously described procedures (chromogenic substrate S-2238).[16] A complete protocol of the binding assay used in this study is also provided.[16b]

Determination of pK_a values: The determination of pK_a values was performed by potentiometric titration following a previously described protocol.[5c]

Determination of log *D* values: The distribution coefficient log *D* was determined by a high-throughput screening method as previously described.[5c]

Calculation of C log *P* values: The C log *P* values were calculated in accordance with the literature.[11b,c]

General procedure A for the fluorination with DAST: A solution of alcohol or ketone (0.13 mmol) in dry CH_2Cl_2 (3 mL) was cooled under Ar to −78 °C before DAST (0.38 mmol) was added. After 15 min, the mixture was warmed to 25 °C and stirred for 2 h. MeOH (2 mL) was added, and the mixture was poured into ice-cold, saturated aqueous $NaHCO_3$ solution, stirred for 30 min, then extracted with CH_2Cl_2. The combined organic phases were dried (Na_2SO_4), the solvent evaporated, and the residue purified by CC (SiO_2; cyclohexane/AcOEt 1:1 or AcOEt).

General procedure B for the methylation of an alcohol with MeI: Method A: A suspension of the alcohol (0.74 mmol) and NaH (1.48 mmol; as a 60% dispersion in mineral oil) in dry THF (3 mL) was stirred under Ar for 1 h at 25 °C. Then MeI (1.11 mmol) was added, and the mixture was stirred for 2 h. Solutions of saturated aqueous LiCl (5 mL) and saturated aqueous NH_4Cl (5 mL) were added, and the mixture was extracted with CH_2Cl_2. The combined organic phases were dried (Na_2SO_4), the solvent evaporated in vacuo, and the residue purified by CC (SiO_2; cyclohexane/AcOEt 1:1, then AcOEt). **Method B**: NaH (1.06 mmol; as a 60% dispersion in mineral oil) was slowly added over 40 min to a solution of the alcohol (0.71 mmol), MeI (1.06 mmol), and [18]crown-6 (1.28 mmol) in dry THF (5 mL), and the mixture was stirred at 25 °C for 2 h. Saturated aqueous NH_4Cl was added and the mixture extracted with AcOEt, the combined organic phases dried (Na_2SO_4), the solvent evaporated in vacuo, and the residue purified by CC (SiO_2; CH_2Cl_2/AcOEt 2:1).

General procedure C for the oxidation of an alcohol with Dess–Martin periodinane: The alcohol (0.74 mmol) was dissolved in dry CH_2Cl_2 (1 mL) under Ar, then Dess–Martin periodinane (1.48 mmol, as a 15% solution in CH_2Cl_2) was added dropwise over 5 min. The mixture was stirred for 3 h at 25 °C before saturated aqueous $NaHCO_3$ and 10% aqueous $Na_2S_2O_3$ were added, and the mixture was extracted with CH_2Cl_2. The organic phase was dried (Na_2SO_4), the solvent evaporated in vacuo, and the residue purified by CC (SiO_2; cyclohexane/AcOEt 1:1).

General procedure D for the preparation of amidinium salts by the pinner reaction: Dry HCl gas was bubbled at 0 °C for 10 min into a solution of the nitrile (0.06 mmol) in dry CH_2Cl_2 (0.5 mL) and dry MeOH (1.0 mL). The mixture was stored at 4 °C for 28–35 h, then the solvent was removed in vacuo. The residue was precipitated with Et_2O, filtered, dried in high vacuum, then dissolved in a solution of NH_3 (2 mL, 7 N in MeOH), and stirred for 3 h at 65 °C. The solvent was evaporated in vacuo, and the residue was purified by CC (SiO_2; CH_2Cl_2/MeOH 9:1).

(3a*S*,4*R*,8*S*,8a*R*,8b*R*)- and (3a*R*,4*R*,8*S*,8a*R*,8b*S*)-4-(4-Bromophenyl)-2-(4-fluorobenzyl)-8-hydroxyhexahydropyrrolo[3,4-*a*]pyrrolizine-1,3-dione ((+)-22 and (−)-23): Compounds **18** (10.43 g, 51 mmol), **19** (9.88 g, 53 mmol), and **20** (7.00 g, 53 mmol) were dissolved in MeCN (80 mL) and stirred under reflux at 80 °C for 18 h. The solvent was evaporated in vacuo, and the residue was purified by CC (SiO_2; AcOEt/pentane 7:3) to give (+)-**22** in 24% and (−)-**23** in 30% yield.

Data for (+)-22: Colorless solid; mp: 123–125 °C; $[\alpha]_D^{25} = +152.2$ ($c = 0.5$, $CHCl_3$); ^1H NMR (500 MHz, $CDCl_3$): $\delta = 7.34$, 7.03 (AA′BB′, $J =$ 8.4 Hz, 4H), 7.26–7.24 (*m*, 2H), 6.96 (t, $J = 8.7$ Hz, 2H), 4.47 (s, 2H), 4.32 (AB, $J = 7.4$ Hz, 1H), 4.04 (d, $J = 8.3$ Hz, 1H), 3.56 (dd, $J = 7.4$, 1.3 Hz, 1H), 3.50 (t, $J = 8.3$ Hz, 1H), 3.45 (dd, $J = 8.3$, 1.3 Hz, 1H), 3.16–3.10 (m, 1H), 2.82–2.69 (br. s, 1H), 2.63–2.58 (m, 1H), 2.43–2.35 (m, 1H), 1.78–1.72 ppm (m, 1H); ^{13}C NMR (125 MHz, $CDCl_3$): $\delta = 177.8$, 174.6, 162.4 (d, $J = 246.7$ Hz), 136.6, 131.3 (d, $J = 3.5$ Hz), 131.3, 130.8 (d, $J = 8.2$ Hz), 129.4, 121.7, 115.3 (d, $J = 21.4$ Hz), 76.2, 75.1, 69.7, 50.4, 49.3, 48.0, 41.8, 33.1 ppm; ^{19}F NMR (282 MHz, $CDCl_3$): $\delta = -114.2$ ppm (m, 1F); IR: $\tilde{\nu} = 2358$, 1688, 1511, 1399, 1350, 1222, 1164, 1091, 1006 cm^{-1}; HRMS (MALDI): calcd for $C_{22}H_{21}BrFN_2O_3^+$ ($[M+H]^+$): 459.0714; found: 459.0708, elemental analysis calcd (%) for $C_{22}H_{20}BrFN_2O_3$: C 57.53, H 4.39, N 6.10, found: C 57.34, H 4.54, N 6.37.

Data for (−)-23: Colorless solid. mp: 56–58 °C; $[\alpha]_D^{25} = -13.4$ ($c =$ 0.5, $CHCl_3$); ^1H NMR (500 MHz, $CDCl_3$): $\delta = 7.47$, 7.30 (AA′BB′, $J =$ 8.6 Hz, 4H), 7.42–7.39 (m, 2H), 7.02 (t, $J = 8.7$ Hz, 2H), 4.64 (s, 2H), 4.09 (dd, $J = 14.7$, 7.2 Hz, 1H), 3.85 (d, $J = 6.8$ Hz, 1H), 3.72 (dd, $J =$ 9.2, 7.2 Hz, 1H), 3.65 (t, $J = 9.2$ Hz, 1H), 3.27 (dd, $J = 9.2$, 6.8 Hz, 1H), 3.14–3.10 (m, 1H), 2.65–2.52 (br. s, 1H), 2.44–2.39 (m, 1H), 2.13–2.07 (m, 1H), 1.87–1.80 ppm (m, 1H); ^{13}C NMR (125 MHz, $CDCl_3$): $\delta = 177.3$, 176.7, 162.6 (d, $J = 247.5$ Hz), 140.2, 131.8, 131.1 (d, $J =$ 3.3 Hz), 130.9 (d, $J = 8.3$ Hz), 128.5, 121.7, 115.7 (d, $J = 21.6$ Hz), 72.8, 72.2, 71.0, 55.4, 50.0, 46.8, 41.9, 33.8 ppm; ^{19}F NMR (282 MHz, $CDCl_3$): $\delta = -114.3$ ppm (m, 1F); IR: $\tilde{\nu} = 2358$, 1692, 1509, 1486, 1394, 1339, 1221, 1157, 1096, 1009 cm^{-1}; HRMS (MALDI): calcd for $C_{22}H_{21}BrFN_2O_3^+$ ($[M+H]^+$): 459.0714, found: 459.0708; elemental analysis calcd (%) for $C_{22}H_{20}BrFN_2O_3$: C 57.53, H 4.39, N 6.10, found: C 57.34, H 4.53, N 6.22.

4-(3a*S*,4*R*,7*R*,8a*S*,8b*R*)- and 4-(3a*R*,4*S*,7*R*,8a*R*,8b*S*)-(4-Bromophenyl)-7-(*tert*-butyldimethylsilanyloxy)-2-(4-fluorobenzyl)hexahydropyrrolo[3,4-*a*]pyrrolizin-1,3-dione ((+)-28 and (−)-29): Compounds **18** (3 g, 14.6 mmol), **19** (2.7 g, 14.6 mmol), and **21** (1.91 g, 14.6 mmol) in DMF (30 mL) were stirred under reflux at 80 °C for 48 h, then the solvent was evaporated in vacuo, and the two pairs of pseudoenantiomers were separated by CC (SiO_2; CH_2Cl_2/AcOEt 1:1), giving *endo*,*trans*-(+)-**24**/(−)-**25** in 47% and *exo*,*trans*-(+)-**26**/(−)-**27** in 35% yield. The *endo*,*trans*-adducts (+)-**24**/(−)-**25** (3.14 g, 6.8 mmol), DMAP (8 mg, 0.07 mmol), TBDMSCl (1.24 g, 8.2 mmol), and NEt_3 (830 mg, 1.2 mL, 8.2 mmol), were dissolved in dry CH_2Cl_2 (20 mL) and stirred under Ar for 35 h at 25 °C. Saturated aqueous $NaHCO_3$ was then added, and the mixture was extracted with CH_2Cl_2. The residue was purified by CC (SiO_2; cyclohexane/AcOEt 4:1) to give (+)-**28** in 31% and (−)-**29** in 42% yield.

Data for (+)-28: Orange solid. mp: 65–67 °C; $[\alpha]_D^{25} = +79.6$ ($c = 1$, $CHCl_3$); ^{1}H NMR (300 MHz, $CDCl_3$): $\delta = 7.36$, 7.05 (AA′BB′, $J = 8.4$ Hz, 4H), 7.32–7.25 (m, 2H), 6.97 (t, $J = 8.8$ Hz, 2H), 4.50 (s, 2H), 4.55–4.44 (m, 1H), 4.08 (dd, $J = 11.4$, 6.2 Hz, 1H), 3.93 (d, $J = 8.8$ Hz, 1H), 3.42 (dd, $J = 8.5$, 8.2 Hz, 1H), 3.24 (dd, $J = 8.0$, 0.8 Hz, 1H), 2.89 (dd, $J = 13.5$, 6.0 Hz, 1H), 2.73 (dd, $J = 13.5$, 3.0 Hz, 1H), 2.01 (d, $J = 12.9$, 6.3 Hz, 1H), 1.92–1.80 (m, 1H), 0.85 (s, 9H), 0.02 (s, 3H), −0.01 ppm (s, 3H); ^{13}C NMR (75 MHz, $CDCl_3$): $\delta = 177.9$, 175.1, 162.7 (d, $J = 247.2$ Hz), 136.9, 131.8, 131.5, 131.1 (d, $J = 8.0$ Hz), 129.9, 121.9, 115.6 (d, $J = 21.3$ Hz), 72.9, 70.0, 66.2, 62.1, 50.6, 48.5, 42.0, 40.4, 26.0, 18.3, −4.6 ppm; ^{19}F NMR (282 MHz, $CDCl_3$): $\delta = -114.5$ ppm (m, 1F); IR: $\tilde{\nu} = 2946$, 2930, 2879, 2855, 1776, 1699, 1604, 1510, 1486, 1471, 1470, 1431, 1396, 1341, 1299, 1250, 1222, 1170, 1090, 1070, 1054, 1009 cm^{-1}; HRMS (MALDI): calcd for $C_{28}H_{35}BrFN_2O_3Si^+$ ($[M+H]^+$): 573.1579, found: 573.1589.

Data for (−)-29: Orange solid. mp: 54–57 °C; $[\alpha]_D^{25} = -88.4$ ($c = 1$, $CHCl_3$); ^{1}H NMR (300 MHz, $CDCl_3$): $\delta = 7.33$, 7.02 (AA′BB′, $J = 8.4$ Hz, 4H), 7.30–7.23 (m, 2H), 6.97 (t, $J = 8.7$ Hz, 2H), 4.72 (d, $J = 9.0$ Hz, 1H), 4.48 (s, 2H), 4.51–4.41 (m, 1H), 3.79 (t, $J = 8.7$ Hz, 1H), 3.56 (t, $J = 8.4$ Hz, 1H), 3.33 (dd, $J = 8.1$, 0.9 Hz, 1H), 2.91 (dd, $J = 13.4$, 5.9 Hz, 1H), 2.62 (dd, $J = 13.4$, 0.3 Hz, 1H), 2.56–2.45 (m, 1H), 1.83–1.72 (m, 1H), 0.84 (t, $J = 2.8$ Hz, 9H), 0.02 (s, 3H), −0.04 ppm (s, 3H); ^{13}C NMR (75 MHz, $CDCl_3$): $\delta = 177.7$, 175.0, 162.3 (d, $J = 245.4$ Hz), 137.0, 131.4, 131.1, 130.8 (d, $J = 8.5$ Hz), 129.6, 121.5, 115.3 (d, $J = 21.9$ Hz), 75.0, 68.8, 67.2, 60.7, 50.5, 50.0, 41.8, 27.0, 25.7, 18.0, −4.7 ppm; ^{19}F NMR (282 MHz, $CDCl_3$): $\delta = -114.4$ ppm (m, 1F); IR: $\tilde{\nu} = 2951$, 2928, 2894, 2856, 1774, 1702, 1604, 1510, 1486, 1472, 1460, 1432, 1396, 1342, 1300, 1282, 1252, 1222, 1170, 1094, 1070, 1050, 1026, 1010 cm^{-1}; HRMS (MALDI): calcd for $C_{28}H_{35}BrFN_2O_3Si^+$ ($[M+H]^+$): 573.1579, found: 573.1588.

(3a*S*,4*R*,7*R*,8a*S*,8b*R*)-4-(4-Bromophenyl)-2-(4-fluorobenzyl)-7-hydroxyhexahydropyrrolo[3,4-*a*]pyrrolizin-1,3-dione ((+)-24): nBu$_4$NF (1.23 mL, 1.23 mmol; as 1 M solution in THF) was added to an ice-cold solution of (+)-**28** (469 mg, 0.82 mmol) in THF (6 mL), and the mixture was stirred for 90 min at 25 °C. The solvent was evaporated in vacuo, and the residue purified by CC (SiO_2; CH_2Cl_2/AcOEt) to give (+)-**24** in 82% yield as a colorless solid. mp: 161–163 °C; $[\alpha]_D^{25} = +107.7$ ($c = 1$, $CHCl_3$); ^{1}H NMR (300 MHz, $CDCl_3$): $\delta = 7.35$, 7.04 (AA′BB′, $J = 8.3$ Hz, 4H), 7.30–7.23 (m, 2H), 6.97 (t, $J = 8.7$ Hz, 2H), 4.64–4.56 (m, 1H), 4.49 (s, 2H), 4.11 (dd, $J = 10.9$, 6.2 Hz, 1H), 3.97 (d, $J = 8.4$ Hz, 1H), 3.46 (dd, $J = 8.4$, 8.1 Hz, 1H), 3.27 (d, $J = 8.1$ Hz, 1H), 2.95 (dd, $J = 13.7$, 6.2 Hz, 1H), 2.78 (dd, $J = 13.7$, 2.8 Hz, 1H), 2.09 (dd, $J = 14.1$, 6.2 Hz, 1H), 1.95 (dd, $J = 11.2$, 6.2 Hz, 1H), 1.73 ppm (d, $J = 3.4$ Hz, 1H); ^{13}C NMR (75 MHz, $CDCl_3$): $\delta = 177.7$, 174.9, 162.6 (d, $J = 246.6$ Hz), 136.7, 131.5, 131.1 (d, $J = 7.9$ Hz), 130.9, 129.8, 122.0, 115.6 (d, $J = 21.4$ Hz), 72.7, 70.1, 66.1, 61.5, 50.6, 48.6, 41.9, 40.2 ppm; ^{19}F NMR (282 MHz, $CDCl_3$): $\delta = -114.4$ ppm (m, 1F); IR: $\tilde{\nu} = 3523$, 2966, 2935, 2910, 2872, 1768, 1693, 1603, 1510, 1486, 1436, 1395, 1344, 1335, 1298, 1260, 1221, 1169, 1158, 1087, 1070, 1039, 1007 cm^{-1}; HRMS (MALDI): calcd for $C_{22}H_{21}BrFN_2O_3^+$ ($[M+H]^+$), 459.0714, found: 459.0706.

4-[(3a*S*,4*R*,8*S*,8a*R*,8b*R*)-2-(4-Fluorobenzyl)-8-hydroxy-1,3-dioxodecahydropyrrolo[3,4-*a*]pyrrolizin-4-yl]benzonitrile ((+)-30): (+)-**22** (2.40 g, 5.24 mmol) and $Zn(CN)_2$ (0.62 g, 5.24 mmol) were added to a suspension of $[Pd_2(dba)_3]$ (0.27 g, 0.29 mmol) and dppf (0.32 g, 0.58 mmol) in DMF (10 mL) under Ar, and the solution was stirred for 16 h at 120 °C. The solvent was evaporated in vacuo and the residue was purified by CC (SiO_2; AcOEt/pentane 5:5, then AcOEt) to give (+)-**30** in 91% yield as a colorless solid. mp: 72–74 °C; $[\alpha]_D^{25} = +122.0$ ($c = 0.5$, $CHCl_3$); ^{1}H NMR (500 MHz, $CDCl_3$): $\delta = 7.51$, 7.28 (AA′BB′, $J = 8.2$ Hz, 4H), 7.28–7.23 (m, 2H), 7.01–6.95 (m, 2H), 4.47 (AB, $J = 14.1$ Hz, 2H), 4.33 (ddd, $J = 13.4$, 8.2, 6.0 Hz, 1H), 4.13 (d, $J = 8.6$ Hz, 1H), 3.58–3.54 (m, 2H), 3.48 (dd, $J = 8.1$, 1.3 Hz, 1H), 3.19–3.14 (m, 1H), 2.86–2.59 (br. s, 1H), 2.62–2.56 (m, 1H), 2.43–2.37 (m, 1H), 1.81–1.74 ppm (m, 1H); ^{13}C NMR (125 MHz, $CDCl_3$): $\delta = 177.5$, 174.4, 162.5 (d, $J = 247.0$ Hz), 143.3, 132.0, 131.3 (d, $J = 3.3$ Hz), 130.8 (d, $J = 8.2$ Hz), 128.5, 118.8, 115.5 (d, $J = 21.5$ Hz), 111.8, 76.2, 75.2, 69.9, 50.5, 49.5, 47.9, 41.9, 33.2 ppm; ^{19}F NMR (282 MHz, $CDCl_3$): $\delta = -114.3$ ppm (m, 1F); IR: $\tilde{\nu} = 3031$, 2354, 1771, 1699, 1510, 1398, 1341, 1171, 1096, 1001 cm^{-1}; HRMS (MALDI): calcd for $C_{23}H_{21}FN_3O_3^+$ ($[M+H]^+$): 406.1561; found, 406.1553; elemental analysis calcd (%) for $C_{23}H_{20}FN_3O_3$: C 68.14, H 4.97, N 10.36, found: C 68.12, H 4.99, N 10.12.

4-[(3a*S*,4*R*,8*R*,8a*R*,8b*R*)-2-(4-Fluorobenzyl)-8-fluoro-1,3-dioxodecahydropyrrolo[3,4-*a*]pyrrolizin-4-yl]benzonitrile ((+)-31): *General procedure A*, starting from (+)-**30** (100 mg, 0.25 mmol) and DAST (127 mg, 0.75 mmol) gave (+)-**31** in 79% yield as a colorless solid. mp: 160–162 °C; $[\alpha]_D^{25} = +206.6$ ($c = 0.5$, $CHCl_3$); ^{1}H NMR (300 MHz, $CDCl_3$): $\delta = 7.50$, 7.28 (AA′BB′, $J = 8.4$ Hz, 4H), 7.28–7.21 (m, 2H), 6.98 (t, $J = 8.7$ Hz, 2H), 5.38–5.34 and 5.16–5.20 (2 × m, 1H), 4.50, 4.45 (AB, $J = 14.0$ Hz, 2H), 4.36 (dd, $J = 8.1$, 0.3 Hz, 1H), 3.77 (dd, $J = 34.8$, 3.0 Hz, 1H), 3.54–3.61 (m, 1H), 3.55 (t, $J = 8.1$, 1H), 3.02–2.91 (m, 1H), 2.80–2.70 (m, 1H), 2.43–2.03 ppm (m, 2H); ^{13}C NMR (125 MHz, $CDCl_3$): $\delta = 177.2$, 174.4, 162.2 (d, $J = 246.6$ Hz), 143.9, 131.8, 131.5 (d, $J = 3.0$ Hz), 130.7 (d, $J = 7.9$ Hz), 128.3, 118.7, 115.3 (d, $J = 21.3$ Hz), 111.4, 97.0 (d, $J = 181.2$ Hz), 71.8 (d, $J = 17.7$ Hz), 70.6, 51.3, 49.5, 44.8 (d, $J = 7.9$ Hz), 41.8, 32.5 ppm (d, $J = 22.0$ Hz); ^{19}F NMR (282 MHz, $CDCl_3$): $\delta = -177.5$ (m, 1F), −113.4 ppm (m, 1F); IR: $\tilde{\nu} = 2961$, 2226, 1776, 1704, 1607, 1511, 1432, 1398, 1344, 1300, 1222, 1172, 1094, 1018 cm^{-1}; HRMS (MALDI): calcd for $C_{23}H_{20}F_2N_3O_2^+$ ($[M+H]^+$): 408.1518, found: 408.1522.

4-[(3a*S*,4*R*,8*S*,8a*R*,8b*R*)-2-(4-Fluorobenzyl)-8-methoxy-1,3-dioxodecahydropyrrolo[3,4-*a*]pyrrolizin-4-yl]benzonitrile ((+)-32): *General procedure B*, *Method A*, starting from (+)-**30** (300 mg, 0.74 mmol), MeI (70 μL, 1.11 mmol), and NaH (59 mg, 1.48 mmol; as a 60% dispersion in mineral oil) gave (+)-**32** in 27% yield as a colorless solid. mp: 55–57 °C; $[\alpha]_D^{25} = +160.7$ ($c = 0.5$, $CHCl_3$); ^{1}H NMR (500 MHz, $CDCl_3$): $\delta = 7.52$, 7.28 (AA′BB′, $J = 8.3$ Hz, 4H), 7.30–7.24 (m, 2H), 7.01–6.95 (m, 2H), 4.51, 4.45 (AB, $J = 14.0$ Hz, 2H), 4.10 (d, $J = 8.4$ Hz, 1H), 3.91–3.87 (m, 1H), 3.67 (dd, $J = 6.6$, 1.4 Hz, 1H), 3.53 (t, $J = 8.4$ Hz, 1H), 3.45 (dd, $J = 8.4$, 1.4 Hz, 1H), 3.43 (s, 3H), 3.13–3.07 (m, 1H), 2.64–2.59 (m, 1H), 2.35–2.28 (m, 1H), 1.82–1.76 ppm (m, 1H); ^{13}C NMR (125 MHz, $CDCl_3$): $\delta = 176.9$, 174.4, 162.5 (d, $J = 246.9$ Hz), 143.3, 132.0, 131.4 (d, $J = 3.3$ Hz), 130.9 (d, $J = 8.2$ Hz), 128.5, 118.8, 115.4 (d, $J = 21.5$ Hz), 111.7, 85.6, 73.5, 69.2, 57.8, 50.5, 49.4, 48.7, 41.8, 29.8 ppm; ^{19}F NMR (282 MHz, $CDCl_3$): $\delta = -114.2$ ppm (m, 1F); IR: $\tilde{\nu} = 2938$, 2359, 2227, 1771, 1699, 1608, 1511, 1398, 1342, 1221, 1171, 1098 cm^{-1}; HRMS

(MALDI): calcd for $C_{24}H_{23}FN_3O_3^+$ ([*M*+H]$^+$): 420.1718; found, 420.1725; elemental analysis calcd (%) for $C_{24}H_{22}FN_3O_3$: C 68.72, H 5.29, N 10.02, found: C 68.85, H 5.21, N 9.86.

4-[(3a*S*,4*R*,8a*R*,8b*R*)-2-(4-Fluorobenzyl)-1,3,8-trioxodecahydropyrrolo[3,4-*a*]pyrrolizin-4-yl]benzonitrile ((+)-33): *General procedure C*, starting from (+)-**30** (300 mg, 0.74 mmol) and Dess–Martin periodinane (4.2 mL, 1.48 mmol) gave (+)-**33** in 63% yield as a red solid. mp: 82–84 °C; $[\alpha]_D^{25} = +266.5$ ($c = 0.5$, $CHCl_3$); ^{1}H NMR (400 MHz, $CDCl_3$): $\delta = 7.57$, 7.32 (AA′BB′, $J = 8.3$ Hz, 4H), 7.33–7.25 (m, 2H), 7.02–6.96 (m, 2H), 4.52, 4.46 (AB, $J = 14.4$ Hz, 2H), 3.97 (d, $J = 8.4$ Hz, 1H), 3.80 (s, 1H), 3.59 (dd, $J = 8.4$ Hz, 1.4, 1H), 3.39 (t, $J = 8.4$, 1H), 3.41–3.32 (m, 1H), 3.02–2.96 (m, 1H), 2.45–2.40 ppm (m, 2H); ^{13}C NMR (100 MHz, $CDCl_3$): $\delta = 215.2$, 176.3, 173.7, 162.6 (d, $J = 247.2$ Hz), 141.6, 132.2, 131.3 (d, $J = 3.4$ Hz), 130.9 (d, $J = 8.2$ Hz), 128.7, 118.6, 115.5 (d, $J = 21.5$ Hz), 112.3, 72.1, 67.7, 49.9, 45.1, 44.6, 42.0, 31.3 ppm; ^{19}F NMR (282 MHz, $CDCl_3$): $\delta = -114.0$ ppm (m, 1F); IR: $\tilde{\nu} = 2360$, 2227, 1747, 1699, 1608, 1510, 1398, 1342, 1222, 1170, 1138 cm^{-1}; HRMS (MALDI): calcd for $C_{23}H_{19}FN_3O_3^+$ ([*M*+H]$^+$) 404.1405, found: 404.1410.

4-[(3a*S*,4*R*,8a*R*,8b*R*)-2-(4-Fluorobenzyl)-8,8-difluoro-1,3-dioxodecahydropyrrolo[3,4-*a*]pyrrolizin-4-yl]benzonitrile ((+)-34): *General procedure A*, starting from (+)-**33** gave (+)-**34** in 48% yield as a colorless solid. mp: 159–161 °C; $[\alpha]_D^{25} = +244.7$ ($c = 0.25$, CH_2Cl_2); ^{1}H NMR (300 MHz, $CDCl_3$): $\delta = 7.50$, 7.24 (AA′BB′, $J = 8.3$ Hz, 4H), 7.28–7.20 (m, 2H), 6.99 (dd, $J = 8.7$, 8.4 Hz, 2H), 4.51, 4.45 (AB, $J = 13.7$ Hz, 2H), 4.31 (dd, $J = 8.1$, 3.1 Hz, 1H); 3.95 (dd, $J = 22.3$, 7.1 Hz, 1H); 3.61–3.51 (m, 2H); 2.26–3.13 (m, 1H); 2.78–2.66 (m, 1H), 2.63–2.23 ppm (m, 2H); ^{13}C NMR (125 MHz, $CDCl_3$): $\delta = 176.4$, 174.2, 162.8 (d, $J = 245.9$ Hz), 142.7, 132.3, 131.5 (d, $J = 3.3$ Hz), 131.2 (d, $J = 8.1$ Hz), 131.1 (dd, $J = 260.0$, 252.8 Hz), 128.7, 118.8, 115.7 (d, $J = 21.4$ Hz), 112.3, 71.8 (dd, $J = 29.7$, 22.2 Hz), 69.1, 50.8, 46.9 (dd, $J = 7.1$, 3.5 Hz), 44.6 (d, $J = 6.2$ Hz), 42.2; 33.8 ppm (dd, $J = 26.2$, 24.8 Hz); ^{19}F NMR (282 MHz, $CDCl_3$): $\delta = -113.9$ (m, 1F), -104.7, -103.9 (2 × m, 1F), -95.5, -94.7 ppm (2×m, 1F); IR: $\tilde{\nu} = 2956$, 2227, 1778, 1704, 1608, 1511, 1433, 1398, 1342, 1301, 1268, 1222, 1160, 1119, 1092, 1018 cm^{-1}; HRMS (MALDI): calcd for $C_{23}H_{19}F_3N_3O_2^+$ ([*M*+H]$^+$): 426.1424, found: 426.1420.

4-[(3a*S*,4*R*,8*S*,8a*R*,8b*R*)-2-(4-Fluorobenzyl)-8-hydroxy-1,3-dioxodecahydropyrrolo[3,4-a]pyrrolizin-4-yl]benzamidine hydrochloride ((+)-2): *General procedure D*, starting from(+)-**30** gave (+)-**2** in 66% yield as a yellow solid. mp: 106–108 °C; $[\alpha]_D^{25} = +120.6$ ($c = 0.5$, MeOH); ^{1}H NMR (500 MHz, $(CD_3)_2SO$): $\delta = 9.35$ (br. s, 2H), 9.18 (br. s, 2H), 7.72, 7.39 (AA′BB′, $J = 8.4$ Hz, 4H), 7.22–7.16 (m, 4H), 5.20 (d, $J = 5.3$ Hz, 1H), 4.50, 4.44 (AB, $J = 14.9$ Hz, 2H), 4.26 (d, $J = 8.7$ Hz, 1H), 4.22–4.16 (m, 1H), 3.77 (t, $J = 8.7$ Hz, 1H), 3.57 (d, $J = 8.7$ Hz, 1H), 3.26 (d, $J = 7.0$ Hz, 1H), 3.01–2.95 (m, 1H), 2.42–2.37 (m, 1H), 2.29–2.22 (m, 1H), 1.58–1.51 ppm (m, 1H); ^{13}C NMR (125 MHz, $(CD_3)_2SO$): $\delta = 178.0$, 175.2, 165.3, 161.4 (d, $J = 243.3$ Hz), 145.5, 132.2 (d, $J = 3.0$ Hz), 129.7 (d, $J = 8.3$ Hz), 128.4, 127.5, 126.5, 115.2 (d, $J = 21.4$ Hz), 74.4, 74.1, 68.8, 50.2, 48.8, 47.5, 40.7, 32.6 ppm; ^{19}F NMR (282 MHz, CD_3OD): $\delta = -115.0$ ppm (m, 1F); IR: $\tilde{\nu} = 3051$, 2359, 1771, 1698, 1510, 1398, 1340, 1221, 1174, 1095, 1022, 1001 cm^{-1}; HRMS (MALDI): calcd for $C_{23}H_{24}FN_4O_3^+$ ([*M*+H]$^+$): 423.1827, found: 423.1825.

4-[(3a*S*,4*R*,8*R*,8a*R*,8b*R*)-2-(4-Fluorobenzyl)-8-fluoro-1,3-dioxodecahydropyrrolo[3,4-*a*]pyrrolizin-4-yl]benzamidine Hydrochloride ((+)-7): *General procedure D*, starting from (+)-**31** gave (+)-**7** in 58% yield as a brown solid. mp: 190–192 °C; $[\alpha]_D^{25} = +209.1$ ($c = 0.25$, CH_3OH); ^{1}H NMR (300 MHz, CD_3OD): $\delta = 9.15$ (m, 2H), 8.70 (m, 2H), 7.83, 7.38 (AA′BB′, $J = 8.0$ Hz, 4H), 7.15 (dd, $J = 8.5$, 5.2 Hz, 2H), 6.95 (dd, $J = 8.8$, 8.5 Hz, 2H), 5.34–5.29 and 5.16–5.10 (2 × m, 1H), 4.50, 4.41 (AB, $J = 14.4$ Hz, 2H), 4.34 (d, $J = 6.6$, 1H), 3.79–3.44 (m, 3H), 2.90–2.79 (m, 1H), 2.70–2.57 (m, 1H), 2.33–1.99 ppm (m, 2H); ^{13}C NMR (75 MHz, CD_3OD): $\delta = 178.7$, 175.9, 167.2, 162.7 (d, $J = 245.0$ Hz), 146.3, 132.2 (d, $J = 3.3$ Hz), 130.4 (d, $J = 8.3$ Hz), 129.0, 127.4, 127.2, 115.0 (d, $J = 21.8$ Hz), 97.4 (d, $J = 180.6$ Hz), 72.1 (d, $J = 17.5$ Hz), 70.8 (d, $J = 2.9$), 51.8, 49.4, 45.0 (d, $J = 8.1$), 41.3, 32.1 ppm (d, $J = 22.3$ Hz); ^{19}F NMR (282 MHz, CD_3OD): $\delta = -177.4$ (m, 1F); -114.8 ppm (m, 1F); IR: $\tilde{\nu} = 3054$, 1775, 1701, 1675, 1614, 1540, 1510, 1489, 1432, 1399, 1344, 1222, 1173, 1095, 1017 cm^{-1}; HRMS (MALDI): calcd for $C_{23}H_{23}F_2N_4O_2^+$ ([*M*+H]$^+$): 425.1784, found: 425.1780.

4-[(3a*S*,4*R*,8*S*,8a*R*,8b*R*)-2-(4-Fluorobenzyl)-8-methoxy-1,3-dioxodecahydropyrrolo[3,4-*a*]pyrrolizin-4-yl]benzamidine hydrochloride ((+)-3): *General procedure D*, starting from (+)-**32** gave (+)-**3** in 56% yield as a brown solid. mp: 155–157 °C; $[\alpha]_D^{25} = +136.8$ ($c = 0.5$, CH_3OH); ^{1}H NMR (300 MHz, CD_3OD): $\delta = 7.63$, 7.42 (AA′BB′, $J = 8.2$ Hz, 4H), 7.29–7.23 (m, 2H), 7.08–7.01 (m, 2H), 4.50, 4.43 (AB, $J = 14.6$ Hz, 2H), 4.30 (d, $J = 8.4$ Hz, 1H), 4.07–3.96 (m, 1H), 3.74 (t, $J = 8.4$ Hz, 1H), 3.61 (dd, $J = 8.4$, 1.2 Hz, 1H), 3.57 (dd, $J = 9.3$, 1.2 Hz, 1H), 3.43 (s, 3H), 3.10–3.00 (m, 1H), 2.66–2.58 (m, 1H), 2.45–2.32 (m, 1H), 1.77–1.67 ppm (m, 1H); ^{13}C NMR (75 MHz, CD_3OD): $\delta = 179.0$, 176.4, 167.7, 162.4 (d, $J = 244.1$ Hz), 146.4, 132.9, 131.0 (d, $J = 8.5$ Hz), 129.7, 128.1, 115.8 (d, $J = 22.0$ Hz), 86.4, 74.8, 69.7, 57.7, 51.7, 42.1, 30.3 ppm; ^{19}F NMR (282 MHz, CD_3OD): $\delta = -114.6$ ppm (m, 1F); IR: $\tilde{\nu} = 3057$, 2359, 1772, 1696, 1675, 1612, 1509, 1398, 1342, 1220, 1174, 1098 cm^{-1}; HRMS (MALDI): calcd for $C_{24}H_{26}FN_4O_3^+$ ([*M*+H]$^+$): 437.1983, found: 437.1985.

4-[(3a*S*,4*R*,8a*R*,8b*R*)-2-(4-Fluorobenzyl)-8,8-difluoro-1,3-dioxodecahydropyrrolo[3,4-*a*]pyrrolizin-4-yl]benzamidine hydrochloride ((+)-8): *General procedure D*, starting from (+)-**34** gave (+)-**8** in 54% yield as a colorless solid. mp: 180–184 °C (dec); $[\alpha]_D^{25} = +207.0$ ($c = 0.25$, CH_3OH); ^{1}H NMR (300 MHz, CD_3OD): $\delta = 7.65$, 7.43 (AA′BB′, $J = 8.4$ Hz, 4H), 7.29–7.22 (m, 2H), 7.06 (t, $J = 8.7$ Hz, 2H), 4.53, 4.46 (AB, $J = 14.7$ Hz, 2H), 4.48 (d, $J = 8.1$ Hz, 1H), 3.93 (dd, $J = 21.8$, 8.0 Hz, 1H), 3.75 (t, $J = 8.4$ Hz, 1H), 3.70 (dd, $J = 8.1$, 6.3 Hz, 1H), 3.27–3.14 (m, 1H), 2.80–2.69 (m, 1H), 2.67–2.50 (m, 1H), 2.48–2.26 ppm (m, 1H); ^{13}C NMR (125 MHz, CD_3OD): $\delta = 176.7$, 174.5, 166.3, 161.8 (d, $J = 245.0$ Hz), 144.1, 131.3 (d, $J = 3.3$ Hz), 130.7 (dd, $J = 256.5$, 254.4 Hz), 129.6 (d, $J = 8.0$ Hz), 128.1, 126.8, 126.7, 114.3 (d, $J = 21.8$ Hz), 71.2 (dd, $J = 30.4$, 22.3 Hz), 67.9, 50.2, 45.8 (d, $J = 6.9$, 4.0 Hz), 43.9 (d, $J = 6.6$ Hz), 40.6, 32.4 ppm (dd, $J = 26.3$, 25.0 Hz); ^{19}F NMR (282 MHz, CD_3OD): $\delta = -114.7$ (m, 1F), -103.4, -102.6 (2×m, 1F), -93.8, -94.6 ppm (2×m, 1F); IR: $\tilde{\nu} = 3052$, 1776, 1703, 1678, 1615, 1539, 1511, 1489, 1433, 1400, 1343, 1301, 1223, 1173, 1162, 1117, 1095 cm^{-1}; HRMS (MALDI): calcd for $C_{23}H_{22}F_3N_4O_2^+$ ([*M*+H]$^+$): 443.1689, found: 443.1685.

4-[(3a*S*,4*R*,8a*R*,8b*R*)-2-(4-Fluorobenzyl)-8,8-dimethoxy-1,3-dioxodecahydropyrrolo[3,4-*a*]pyrrolizin-4-yl]benzamidine hydrochloride ((+)-9): *General procedure D*, starting from (+)-**33** gave (+)-**9** in 31% yield as a brown solid. mp: 186–188 °C; $[\alpha]_D^{25} = +120.6$ ($c = 0.5$, CH_3OH); ^{1}H NMR (300 MHz, CD_3OD): $\delta = 7.64$, 7.43 (AA′BB′, $J = 8.2$ Hz, 4H), 7.28–7.24 (m, 2H), 7.08–7.02 (m, 2H), 4.51, 4.45 (AB, $J = 14.3$ Hz, 2H), 4.43 (d, $J = 8.7$ Hz, 1H), 3.83–3.80 (m, 1H), 3.64–3.58 (m, 2H), 3.39 (s, 3H), 3.34 (s, 3H), 3.07–2.97 (m, 1H), 2.65–2.57 (m, 1H), 2.52–2.44 (m, 1H), 1.88–1.79 ppm (m, 1H); ^{13}C NMR (75 MHz, CD_3OD): $\delta = 179.8$, 176.7, 167.7, 161.3 (d, $J = 245.3$ Hz), 146.5, 133.0, 130.9 (d, $J = 8.5$ Hz), 129.7, 128.1, 123.3, 115.7 (d, $J = 21.9$ Hz), 111.2, 75.5, 69.1, 52.5, 50.0, 46.7, 42.0, 33.8 ppm; ^{19}F NMR (282 MHz, CD_3OD): $\delta = -114.6$ ppm (m, 1F); IR: $\tilde{\nu} = 2953$, 2358, 1774, 1699, 1674, 1615, 1510, 1398, 1340, 1135, 1099, 1042 cm^{-1}; HRMS (MALDI): calcd for $C_{25}H_{28}FN_4O_4^+$ ([*M*+H]$^+$): 467.2089, found: 467.2081.

X-ray analysis: The structures were solved by direct methods (SIR97)[19] and refined by full-matrix least-squares analysis (SHELXL-97)[20] using an isotropic extinction correction. All non-H atoms were refined anisotropically, H atoms isotropically, whereby H positions are based on stereochemical considerations.

X-ray crystal structure of (+)-**39**: Crystal data at 183(2) K for $C_{23}H_{19}F_2N_3O_2$ (M_r = 407.41) orthorhombic, space group $P2_12_12_1$ (no 19), ρ_{calcd} = 1.389 g cm^{-3}, Z = 4, a = 10.4015(3) Å, b = 12.6531(4) Å, c = 14.8005(5) Å, V = 1947.91(11) Å^3. Bruker-Nonius Kappa-CCD diffractometer, $Mo_{K\alpha}$ radiation, λ = 0.7107 Å, μ = 0.103 mm^{-1}. Final $R(F)$ = 0.037, w$R(F^2)$ = 0.085 for 272 parameters and 3408 reflections with $I > 2\sigma(I)$ and $3.74 < \theta < 26.01^\circ$ (corresponding R values based on all 3773 reflections are 0.044 and 0.091, respectively).

X-ray crystal structure of (+)-**22**: Crystal data at 203(2) K for $C_{22}H_{20}BrFN_2O_3$ (M_r = 459.31) monoclinic, space group $P2_1$ (no 4), ρ_{calcd} = 1.416 g cm^{-3}, Z = 2, a = 12.8360(10) Å, b = 5.1640(4) Å, c = 16.2915(10) Å, β = 94.174(4)°, V = 1077.02(14) Å^3. Bruker-Nonius Kappa-CCD diffractometer, $Mo_{K\alpha}$ radiation, λ = 0.7107 Å, μ = 1.941 mm^{-1}. Final $R(F)$ = 0.055, w$R(F^2)$ = 0.146 for 283 parameters and 2727 reflections with $I > 2\sigma(I)$ and $3.50 < \theta < 25.05^\circ$ (corresponding R values based on all 3292 reflections are 0.073 and 0.162, respectively).

X-ray crystal structure of (+)-**34**: Crystal data at 220(2) K for $C_{23}H_{18}F_3N_3O_2$ (M_r = 425.40) monoclinic, space group $C2$ (no 5), ρ_{calcd} = 1.462 g cm^{-3}, Z = 4, a = 21.7419(10) Å, b = 5.1347(2) Å, c = 17.4446(10) Å, β = 97.038(2)°, V = 1932.81(16) Å^3. Bruker-Nonius Kappa-CCD diffractometer, $Mo_{K\alpha}$ radiation, λ = 0.7107 Å, μ = 0.115 mm^{-1}. Final $R(F)$ = 0.044, w$R(F^2)$ = 0.098 for 299 parameters, 1 restraint, and 3150 reflections with $I > 2\sigma(I)$ and $7.03 < \theta < 26.03^\circ$ (corresponding R values based on all 3601 reflections are 0.055 and 0.106, respectively).

X-ray crystal structure of (+)-**36**: Crystal data at 220(2) K for $C_{23}H_{19}F_2N_3O_2$ (M_r = 407.41) orthorhombic, space group $P2_12_12_1$ (no 19), ρ_{calcd} = 1.364 g cm^{-3}, Z = 4, a = 10.9500(2) Å, b = 10.9922(3) Å, c = 16.4856(4) Å, V = 1984.28(8) Å^3. Bruker-Nonius Kappa-CCD diffractometer, $Mo_{K\alpha}$ radiation, λ = 0.7107 Å, μ = 0.101 mm^{-1}. Final $R(F)$ = 0.052, w$R(F^2)$ = 0.138 for 324 parameters and 3801 reflections with $I > 2\sigma(I)$ and $6.44 < \theta < 27.51^\circ$ (corresponding R values based on all 4467 reflections are 0.064 and 0.150, respectively).

CCDC-295279 ((+)-**39**), CCDC-295280 ((+)-**22**), CCDC-295281 ((+)-**34**), and CCDC-295282 ((+)-**36**) contain the supplementary crystallographic data for this paper. These data can be obtained free of charge from The Cambridge Crystallographic Data Centre via www.ccdc.cam.ac.uk/data_request/cif.

Acknowledgements

This research was supported by F. Hoffmann–La Roche Ltd, Chugai Pharmaceuticals, and the ETH Research Council. A.H.-R. thanks the Deutsche Forschungsgemeinschaft (Emmy Noether-Programm), and J.A.O. thanks the Carlsberg Foundation for a postdoctoral fellowship. We thank Olivier Kuster, Dr. Thomas Tschopp, and Dr. Alain Gast for the biological assays.

Keywords: bioisosterism · fluorine · noncovalent interactions · partition coefficient · thrombin inhibitors

[1] a) H.-J. Böhm, D. Banner, S. Bendels, M. Kansy, B. Kuhn, K. Müller, U. Obst-Sander, M. Stahl, *ChemBioChem* **2004**, *5*, 637–643; b) B. K. Park, N. R. Kitteringham, P. M. O'Neill, *Annu. Rev. Pharmacol. Toxicol.* **2001**, *41*, 443–470; c) D. O'Hagan, H. S. Rzepa, *Chem. Commun.* **1997**, 645–652; d) B. E. Smart, *J. Fluorine Chem.* **2001**, *109*, 3–11.

[2] P. Jeschke, *ChemBioChem* **2004**, *5*, 570–589.

[3] For recent journal issues, monographs, and reviews on organofluorine chemistry, see: a) *ChemBioChem* **2004**, *5*, 559–722; b) *Chimia* **2004**, *58*, 92–162; c) *Chimia* **2003**, *57*, 674–734; d) P. Kirsch, *Modern Fluoroorganic Chemistry: Synthesis Reactivity, Applications*, Wiley-VCH, Weinheim, **2004**; e) M. Shimizu, T. Hiyama, *Angew. Chem.* **2005**, *117*, 218–234; *Angew. Chem. Int. Ed.* **2005**, *44*, 214–231; f) K. Mikami, Y. Itoh, M. Yamanaka, *Chem. Rev.* **2004**, *104*, 1–16; g) W. R. Dolbier, Jr., *J. Fluorine Chem.* **2005**, *126*, 157–163.

[4] a) U. Obst, V. Gramlich, F. Diederich, L. Weber, D. W. Banner, *Angew. Chem.* **1995**, *107*, 1874–1877; *Angew. Chem. Int. Ed. Engl.* **1995**, *34*, 1739–1742; b) U. Obst, D. W. Banner, L. Weber, F. Diederich, *Chem. Biol.* **1997**, *4*, 287–295; c) K. Schärer, M. Morgenthaler, P. Seiler, F. Diederich, D. W. Banner, T. Tschopp, U. Obst-Sander, *Helv. Chim. Acta* **2004**, *87*, 2517–2538; d) U. Obst, P. Betschmann, C. Lerner, P. Seiler, F. Diederich, V. Gramlich, L. Weber, D. W. Banner, P. Schönholzer, *Helv. Chim. Acta* **2000**, *83*, 855–909; e) P. Betschmann, S. Sahli, F. Diederich, U. Obst, V. Gramlich, *Helv. Chim. Acta* **2002**, *85*, 1210–1245.

[5] a) J. A. Olsen, D. W. Banner, P. Seiler, U. Obst-Sander, A. D'Arcy, M. Stihle, K. Müller, F. Diederich, *Angew. Chem.* **2003**, *115*, 2611–2615; *Angew. Chem. Int. Ed.* **2003**, *42*, 2507–2511; b) J. A. Olsen, D. W. Banner, P. Seiler, B. Wagner, T. Tschopp, U. Obst-Sander, M. Kansy, K. Müller, F. Diederich, *ChemBioChem* **2004**, *5*, 666–675; c) J. Olsen, P. Seiler, B. Wagner, H. Fischer, T. Tschopp, U. Obst-Sander, D. W. Banner, M. Kansy, K. Müller, F. Diederich, *Org. Biomol. Chem.* **2004**, *2*, 1339–1352.

[6] For a systematic investigation of fluorine substitution in carbonic anhydrase II inhibitors, see: a) C.-Y. Kim, J. S. Chang, J. B. Doyon, T. T. Baird, Jr., C. A. Fierke, A. Jain, D. W. Christianson, *J. Am. Chem. Soc.* **2000**, *122*, 12125–12134; b) R. D. Madder, C.-Y. Kim, P. P. Chandra, J. B. Doyon, T. A. Baird, Jr., C. A. Fierke, D. W. Christianson, J. G. Voet, A. Jain, *J. Org. Chem.* **2002**, *67*, 582–584.

[7] a) R. Paulini, K. Müller, F. Diederich, *Angew. Chem.* **2005**, *117*, 1820–1839; *Angew. Chem. Int. Ed.* **2005**, *44*, 1788–1805; b) F. Hof, D. M. Scofield, W. B. Schweizer, F. Diederich, *Angew. Chem.* **2004**, *116*, 5166–5169; *Angew. Chem. Int. Ed.* **2004**, *43*, 5056–5059.

[8] For related studies on halogenated amidinium residues in the selectivity pocket of serine proteases, see: a) R. L. Mackman, B. A. Katz, J. G. Breitenbucher, H. C. Hui, E. Verner, C. Luong, L. Liu, P. A. Sprengeler, *J. Med. Chem.* **2001**, *44*, 3856–3871; b) B. A. Katz, P. A. Sprengeler, C. Luong, E. Verner, K. Elrod, M. Kirtley, J. Janc, J. R. Spencer, J. G. Breitenbucher, H. Hui, D. McGee, D. Allen, A. Martelli, R. L. Mackman, *Chem. Biol.* **2001**, *8*, 1107–1121.

[9] For C–F, C–OH bioisosterism, see: a) *Organofluorine Chemistry, Principles and Commercial Applications* (Eds.: R. E. Banks, B. E. Smart, J. C. Tatlow), Plenum, New York, **1994**; b) K. Toshima, *Carbohydr. Res.* **2000**, *327*, 15–26; c) J. J. McAtee, R. F. Schinazi, D. C. Liotta, *J. Org. Chem.* **1998**, *63*, 2161–2167; d) S. J. Williams, S. G. Withers, *Carbohydr. Res.* **2000**, *327*, 27–46.

[10] a) L. Moreira Lima, E. J. Barreiro, *Curr. Med. Chem.* **2005**, *12*, 23–49; b) G. A. Patani, E. J. LaVoie, *Chem. Rev.* **1996**, *96*, 3147–3176.

[11] a) C. Hansch, A. Leo, *Exploring QSAR, Fundamentals and Applications in Chemistry and Biology*, ACS, Washington, **1995**; b) A. Leo, C. Hansch, *Perspect. Drug Discovery Des.* **1999**, *17*, 1–25. c) A. J. Leo, D. Hoekman, *Perspect. Drug Discovery Des.* **2000**, *18*, 19–38.

[12] W. J. Middleton, *J. Org. Chem.* **1975**, *40*, 574–578.

[13] a) A. Pinner, F. Klein, *Ber. Dtsch. Chem. Ges.* **1877**, *10*, 1889–1897; b) G. Wagner, I. Wunderlich, *Pharmazie* **1977**, *32*, 76–79.

[14] O. Mitsunobu, *Synthesis* **1981**, 1–28.

[15] a) M. Schlosser, *Angew. Chem.* **1998**, *110*, 1538–1556; *Angew. Chem. Int. Ed.* **1998**, *37*, 1496–1513; b) F. Leroux, P. Jeschke, M. Schlosser, *Chem. Rev.* **2005**, *105*, 827–856.

[16] a) R. Lottenberg, J. A. Hall, M. Blinder, E. P. Binder, C. M. Jackson, *Biochim. Biophys. Acta* **1983**, *742*, 539–557; b) K. Hilpert, J. Ackermann, D. W. Banner, A. Gast, K. Gubernator, P. Hadváry, L. Labler, K. Müller, G. Schmid, T. B. Tschopp, H. van de Waterbeemd, *J. Med. Chem.* **1994**, *37*, 3889–3901.

[17] P. R. Gerber, K. Müller, *J. Comput.-Aided Mol. Des.* **1995**, *9*, 251–268; Gerber Molecular Design (http://www.moloc.ch).

[18] a) W. Bode, I. Mayr, U. Baumann, R. Huber, S. R. Stone, J. Hofsteenge, *EMBO J.* **1989**, *8*, 3467 – 3475; b) D. W. Banner, P. Hadváry, *J. Biol. Chem.* **1991**, *266*, 20085–20093.
[19] A. Altomare, M. C. Burla, M. Camalli , G. L. Cascarano, C. Giacovazzo, A. Guagliardi, A. G. G. Moliterni, G. Polidori, R. Spagna, *J. Appl. Crystallogr.* **1999**, *32*, 115 – 119.
[20] G. M. Sheldrick, *SHELXL-97 Program for the Refinement of Crystal Structures*. University of Göttingen, Germany, **1997**.

Received: January 24, 2006
Published online on April 20, 2006

